

Unified Impedance and Hybrid Force-Position Controller with Kinesthetic Filtering

Antonio Gonzales Marin and Roman Weitschat

Abstract—Interaction control is a mature, but still, current area of research in robotics. Various approaches have been developed for passive and active force regulation and tracking, e.g. impedance control, direct force and hybrid force-position control. The latter method implements a force feedback outer loop on top of a position controller inner loop, where commands are issued with respect to a compliant frame. However, if the compliant frame undergoes a rigid transformation, e.g. in order to specify the same task relative to another reference frame, then commands can be rendered non-compliant with the task at hand. As a consequence, the robot can be damaged or hurt somebody, this is further aggravated by the rigidity of a position controller. In the present paper, we propose a unified impedance and hybrid force-position control scheme to address such issues. The unified controller benefits from the impedance control compliance while an explicit force value can be achieved. Furthermore, we augment the designed controller with a kinesthetic filter, which ensures that the commanded pose and wrench are consistent with a given task model. We validate the designed system through experiments with a lightweight robot (LWR). The proposed approach finds applications in industrial settings where interactions with the environment are required in order to fulfill a task and the system must be robust w.r.t. input commands.

I. INTRODUCTION

In recent years, robotic automation in industry has been oriented towards small and medium-sized enterprises (SME). From the economic point of view the possibility of using a robot as central component of industrial processes allows to reduce production costs, increase manufacturing throughput and the quality of products. From the perspective of occupational safety and health, the workers do not need to engage in repetitive heavy-duty or hazardous labor, which can be handled by a robot. Albeit, there still exist tasks that cannot be fully automated. Such tasks can benefit from the use of a robot, but a human operator needs to be present as well. For example, in an assembly line an operator can be responsible for choosing and placing necessary parts, then a robot can be employed in order to systematically treat the parts, e.g. drilling, deburring or screwing. In such a scenario, human and robot share the same workspace to perform the task. Input parameters to the system can be achieved by an operator or an automatic high-level planner. Therefore, the system that controls the robot must be robust w.r.t. control system parameters and the task at hand, in order not to harm the human operator or the parts being treated. The approach

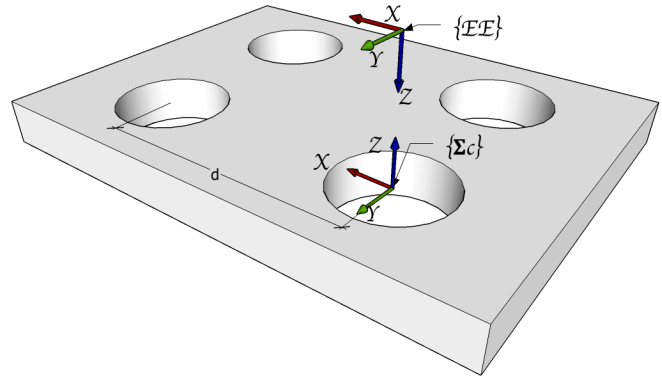


Fig. 1: The compliant frame $\{\Sigma_c\}$ is defined for an insertion task. The robot’s end-effector $\{EE\}$ is force/torque-constrained on $x - y$ plane, while it is free to perform translations and rotations along and about the z -axis direction.

we use in this work is to filter the desired position and wrench values before commanding them to the force/motion control system. In this way the inputs are guaranteed to comply with the given environment and task model.

For the specification of the task it is common to use a compliant frame Σ_c . The motion and wrench commands can be commanded either by an operator or a high-level planner, depending on the task, w.r.t the defined Σ_c . For interaction tasks it is particularly important to ensure that the desired motion and wrench are compliant with each other, otherwise the environment or the robot itself can be damaged, see Fig. 1. In order to enforce this requirement the *selection matrix* $S \in \mathbb{R}^{6 \times 6}$ and its complement $I_6 - S$ can be applied as a filtering technique [2], [3], [4]. When using this approach the task is also characterized relative to the compliant frame. However, if this frame is subject to rigid transformations, when needed, then the commanded wrench and position are not filtered correctly, see Sec. III-C. Hence, a combination of wrench and position commands that was compliant with the task becomes non-compliant, therefore the selection matrix is said to be noninvariant w.r.t. rigid transformations. *Kinesthetic filtering* was presented as a solution to this problem [5]. This formulation is based on the reciprocity property of wrenches and twists jointly with the characterization of the task and proper design of the projective matrices or filters.

Force control schemes were formulated in [6], [7], [8], [9] and [10], these works implement a force feedback loop on top of a generic position control. Hybrid control approaches in [2], [3], [4] and [11] feature the use of selection ma-

All authors are with Robotics and Mechatronics Center (RMC), German Aerospace Center (DLR), 82234 Wessling, Germany.
 {Antonio.GonzalesMarin, Roman.Weitschat}@dlr.de

trices in order to separate wrench and motion subspaces. Recently, a similar approach of force loop and impedance control was presented in [12], where the initialization and supervision of the force control loop are managed through task-energy tanks. In this work, it is implicitly assumed that the commanded wrench and motion are compliant, since no validation is made for such input commands.

We propose a straightforward way of describing the task, see Sec. IV. This permits for the environment description to be abstracted from the end-user while ensuring correctness through automatic and proper generation of the projection matrices. Although we use the kinestatic filtering concept, we apply the redefinition of the projection matrices which was given in [13]. There, the original filter proposed in [4] is utilized with the necessary modifications to yield invariance w.r.t. (1) rigid body transformations, (2) changes in unit length and (3) basis changes. Furthermore, we introduce the concept of selection vector and pragmatical solutions for the implementation of the hybrid force-position controller.

First, we describe the underlying characteristics and physical properties of the system in Sec. II-A. Then, Sec. II-B follows with a brief explanation of the impedance controller and its relevant characteristics to this work, Sec. II-C delineates the force controller structure. In Sec. III the kinestatic filtering problem is stated and in Sec. IV we introduce the *selection vector* abstraction along other pragmatical solutions. In Sec. V validation of the presented approach is supported by simulation and experiment results and in Sec. VI we explain the aim of future developments.

II. ROBOT MODELING

The control scheme was implemented on a DLR Lightweight Robot (LWR4). This lightweight robot is torque-controlled, enables the use of torque feedback for full-state control and has a payload to weight ratio of 1:1 [14]. The structural design is modular and comprises 7 degrees of freedom (DOF).

A. Robot Dynamics

The dynamics inherent to a serial n -DOF flexible-joint robot can be expressed as [15]

$$M(\mathbf{q})\ddot{\mathbf{q}} + C(\mathbf{q}, \dot{\mathbf{q}})\dot{\mathbf{q}} + \mathbf{g}(\mathbf{q}) = \boldsymbol{\tau}_J + \boldsymbol{\tau}_{ext} \quad (1)$$

$$B\ddot{\boldsymbol{\theta}} + \boldsymbol{\tau}_J = \boldsymbol{\tau}_m - \boldsymbol{\tau}_f \quad (2)$$

$$\boldsymbol{\tau}_J = K(\boldsymbol{\theta} - \mathbf{q}) + D(\dot{\boldsymbol{\theta}} - \dot{\mathbf{q}}), \quad (3)$$

In the case of the LWR each joint comprises harmonic gearboxes, for which equations (1)-(3) are valid. Here, \mathbf{q} , $\dot{\mathbf{q}} \in \mathbb{R}^n$ are the link positions and velocities, while $\boldsymbol{\theta}$, $\dot{\boldsymbol{\theta}}$ and $\ddot{\boldsymbol{\theta}}$ are the motor position, velocities and accelerations respectively, $M(\mathbf{q}) \in \mathbb{R}^{n \times n}$ is symmetric positive-definite inertia matrix, $C(\mathbf{q}, \dot{\mathbf{q}})\dot{\mathbf{q}} \in \mathbb{R}^n$ the vector of Coriolis and centrifugal effects and $\mathbf{g}(\mathbf{q}) \in \mathbb{R}^n$ the gravity vector. Matrices $B \in \mathbb{R}^{n \times n}$ and $K \in \mathbb{R}^{n \times n}$ represent the motor inertia and joint stiffness, both are positive definite and constant diagonal matrices, $D \in \mathbb{R}^{n \times n}$ is the diagonal and semi-definite damping matrix. The joint, motor, friction torque

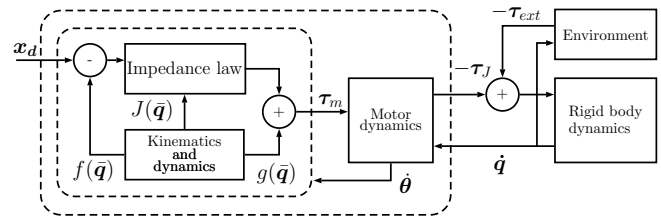


Fig. 2: Overview of the Cartesian impedance controller [17].

vectors and external torque are represented by $\boldsymbol{\tau}_J$, $\boldsymbol{\tau}_m$, $\boldsymbol{\tau}_f$ and $\boldsymbol{\tau}_{ext} \in \mathbb{R}^n$, correspondingly. Based on this preliminary theory, the concept of impedance and force control are explained next.

B. Spatial Impedance Controller

Impedance control regulates the relationship between acceleration, velocity, position and force, such as a mass-spring-damper (virtual) system [16], thus it regulates the mechanical behavior of the system. The impedance behavior of the LWR is achieved by virtue of the available torque sensors. The system full state is defined as $(\boldsymbol{\theta}, \dot{\boldsymbol{\theta}}, \boldsymbol{\tau}, \dot{\boldsymbol{\tau}})$ with the joint position $\boldsymbol{\theta}$ and the joint torques $\boldsymbol{\tau}$ as measured values, as well as their derivatives $\dot{\boldsymbol{\theta}}$, $\dot{\boldsymbol{\tau}}$, which are computed numerically. The controller design follows a passivity-based approach. This is accomplished by means of (1) an auxiliary link position variable $\bar{\mathbf{q}}(\boldsymbol{\theta})$ calculated iteratively using a contraction mapping of the motor positions at an equilibrium point [17], and (2) by adopting a passive impedance law such as the one described in [18]. The auxiliary variable ensures that the position feedback depends on the measured motor position vector $\boldsymbol{\theta}$ only, but is equivalent to the link-side position vector \mathbf{q} . On the other hand, the impedance law provides a means to regulate the energy that is injected to the system by changing internal geometrical properties of the virtual spring. The torques applied to the motors are characterized by a spring-damper response with gravity compensation

$$\boldsymbol{\tau}_m = \boldsymbol{\tau}_{ic} \quad (4)$$

$$\boldsymbol{\tau}_{ic} = -J^T(\bar{\mathbf{q}}) \left(K_x \tilde{\mathbf{x}}(\bar{\mathbf{q}}) + D_x J(\bar{\mathbf{q}}) \dot{\boldsymbol{\theta}} + \mathbf{g}(\bar{\mathbf{q}}) \right) \quad (5)$$

$$\tilde{\mathbf{x}}(\bar{\mathbf{q}}) = \mathbf{f}(\bar{\mathbf{q}}) - \mathbf{x}_d, \quad (6)$$

where $J(\bar{\mathbf{q}})$ is the Jacobian associated with the static link-side positions $\bar{\mathbf{q}}$, $K_x, D_x \in \mathbb{R}^{6 \times 6}$ are the Cartesian stiffness and damping matrices that define the impedance behavior of the robot, $\tilde{\mathbf{x}}(\bar{\mathbf{q}})$ is the Cartesian position error defined through the forward kinematics $\mathbf{f}(\bar{\mathbf{q}})$ and the desired Cartesian position \mathbf{x}_d , whereas $\mathbf{g}(\bar{\mathbf{q}})$ is added for gravity compensation purposes. The structural overview of the impedance controller is shown in Fig. (2).

C. Hybrid Force-Position Controller

The hybrid force-position control scheme combines information of two reciprocal subspaces: twists and wrenches for tracking a desired interaction wrench and simultaneously perform a motion command. The chosen force controller

exhibits a proportional-integral action, since it has been shown that an integral component provides stable system behavior even for high-stiffness contacts [19]. The controller is defined as

$$\Delta_f(t) = \mathfrak{F}_{ext}(t) - \mathfrak{F}_d(t) \quad (7)$$

$$\mathfrak{F}_i(t) = \begin{bmatrix} \mathbf{f}_i \\ \mathbf{m}_i \end{bmatrix} \quad (8)$$

$$\tau_{fc} = J^T(\bar{q}) \left[K_p \Delta_f + K_i \int \Delta_f dt \right], \quad (9)$$

where $\mathfrak{F}_{ext} = (\mathbf{f}_{ext}^T, \mathbf{m}_{ext}^T)$ is the wrench acting on the robot from the environment side and is measured by a 6-DOF force-torque sensor mounted on the wrist of the robot. The vector $\mathfrak{F}_d = (\mathbf{f}_d^T, \mathbf{m}_d^T)$ represents the desired wrench that the robot is commanded to exert for a given task and $\Delta_f(t)$ is the force error signal. Then, the input to the system is a combined response of the impedance and force controllers

$$\tau_m = \tau_{ic} + \tau_{fc}, \quad (10)$$

where torques generated by the force control law τ_{fc} are superimposed to the impedance controller torques τ_{ic} . As mentioned above, the desired motion and force have to be in agreement and reflect valid constraints imposed by the interaction task with the environment. We realize this by means of kinestatic filtering as explained in the next section.

III. KINESTATIC FILTERING

A. Twist and wrench decomposition

In classical hybrid force-position control methods, the separation of force and position subspaces is achieved by means of the selection matrix S , for position, and its complement $I_6 - S$, for force. This matrix is diagonal with binary entries $S = \text{diag}(s_i)$, $s_i = \{1, 0\}$ where $i = \overline{1, n}$, and a “1” in S indicates that the corresponding axis is position-controlled, otherwise force-controlled. This formulation of the hybrid control using selection matrices may lead to unexpected results when the compliant frame is translated. To overcome this limitation the kinestatic filtering approach was proposed in [5]. The basic idea of this method lies on the possibility of decomposing twist and wrench spaces into consistent and inconsistent subspaces

$$H = [B \ \bar{B}] \quad (11)$$

$$g = [a \ \bar{a}] \quad (12)$$

where H , g are the twist and wrench spaces that comprise the inconsistent \bar{B} , \bar{a} and consistent B , a subspaces. The desired twist and wrench can be projected onto the latter subspaces by appropriate design of filters, or projection matrices. As a result, the inconsistent parts \bar{B} and \bar{a} are filtered out. The filters are defined as

$$P_B^{kin} = B(B^T \Psi B)^{-1} B^T \Psi, \quad P_a^{kin} = a(a^T \psi a)^{-1} a^T \psi \quad (13)$$

$$\mathbf{T}_B = P_B^{kin} \mathbf{T}, \quad \mathbf{w}_a = P_a^{kin} \mathbf{w}, \quad (14)$$

where matrices B and a are the consistent twist and wrench subspaces, and represent one of the possible twist/wrench

combinations compliant with the environment model. The commanded twist \mathbf{T} and wrench \mathbf{w} are projected to the consistent twist and wrench subspaces by filters P_B^{kin} and P_a^{kin} respectively, and $\Psi = \psi = \Delta = \begin{bmatrix} \mathbf{0} & I_3 \\ I_3 & \mathbf{0} \end{bmatrix}$ embody the twist and wrench metrics. Both equations in (14) satisfy the vanishing criteria of instantaneous work $\mathbf{T}_B^T \mathbf{w}_a = 0$ and thus are consistent.

Under a transformation K , for motion, and G , for wrench, the following relations must be satisfied

$$\Psi' = K^{-T} \Psi K^{-1}, \quad \psi' = G^{-T} \psi G^{-1}, \quad (15)$$

i.e. the metrics account for the transformation $\Psi' \neq \Psi$ and $\psi' \neq \psi$. In this context, if the redefinition of metric matrices is explicitly taken as $\Psi = \psi = I_6$, then the approach can be applied no matter what metric is being used [13].

B. Modified kinestatic filtering

Kinestatic filtering is based on the geometric description of motion and force by means of twists and wrenches, while homogeneous transformations are the more ubiquitous way of representing motion and are used in this implementation. To get around this problem, the subspace B can be defined as a linear combination of elementary motion vectors $\mathbf{T}_i \in \mathbb{R}^6$, where only element $t_i = 1$ for \mathbf{T}_i , i.e. $\mathbf{T}_5 = [0 \ 0 \ 0 \ 0 \ 1 \ 0]^T$. Also, the rotational components need to be scaled appropriately by a constant factor with length dimensions p , namely $\omega' = p\omega$, $\tau' = \tau/p$ [4]. We denominate this representation of the stack vector of a position and a rotation vector pseudo-twist

$$\mathbf{T} = \begin{bmatrix} p_x \\ p_y \\ p_z \\ \omega'_x \\ \omega'_y \\ \omega'_z \end{bmatrix}, \quad \mathbf{w} = \begin{bmatrix} f_x \\ f_y \\ f_z \\ \tau'_x \\ \tau'_y \\ \tau'_z \end{bmatrix}, \quad (16)$$

where $\mathbf{p} = [p_x \ p_y \ p_z]^T$ is the displacement vector and ω holds the axis and angle of rotation, associated with a desired Euler angle¹ rotation matrix R_d . The former values are obtained from a desired homogeneous transformation $g_d = \left[\begin{array}{c|c} R_d & \mathbf{p}_d \\ \hline \mathbf{0}_{3 \times 1} & 1 \end{array} \right]$. Hereafter, pseudo-twists are used along the kinestatic filtering instead of the formal twist definition.

C. Invariance of the Hybrid Force-Position Control

The following example shows the invariance and noninvariance of the kinestatic filtering and the selection matrix and is based on the approach presented in [13]. For an insertion task, one possible definition of the environment

¹In our system, Euler angle representations are used for commands and visual feedback while all the calculations, e.g. rotational interpolation, involve quaternions.

model via matrices B and a is as follows

$$B = \begin{bmatrix} 0 & 0 \\ 0 & 0 \\ 1 & 0 \\ 0 & 0 \\ 0 & 0 \\ 0 & 1 \end{bmatrix}, \quad a = \begin{bmatrix} 1 & 0 & 0 & 0 \\ 0 & 1 & 0 & 0 \\ 0 & 0 & 1 & 0 \\ 0 & 0 & 0 & 1 \\ 0 & 0 & 0 & 0 \\ 0 & 0 & 0 & 0 \end{bmatrix}. \quad (17)$$

Here, B describes a translation along z -axis and a rotation about the same axis, matrix a allows the specification of a wrench on the $x - y$ plane. Matrix B spans all the possible elementary motions, for this task, namely $B = \{\mathbf{T}_3, \mathbf{T}_6\}$.

The filters suggested in [3] for the same task are defined as

$$P_B = I_6 - S = \begin{bmatrix} 0 & 0 & 0 & 0 & 0 & 0 \\ 0 & 0 & 0 & 0 & 0 & 0 \\ 0 & 0 & 1 & 0 & 0 & 0 \\ 0 & 0 & 0 & 0 & 0 & 0 \\ 0 & 0 & 0 & 0 & 0 & 0 \\ 0 & 0 & 0 & 0 & 0 & 1 \end{bmatrix}, \quad P_a = S = \begin{bmatrix} 1 & 0 & 0 & 0 & 0 & 0 \\ 0 & 1 & 0 & 0 & 0 & 0 \\ 0 & 0 & 0 & 0 & 0 & 0 \\ 0 & 0 & 0 & 1 & 0 & 0 \\ 0 & 0 & 0 & 0 & 1 & 0 \\ 0 & 0 & 0 & 0 & 0 & 0 \end{bmatrix}. \quad (18)$$

If the compliant frame undergoes a rigid transformation, then the filters become

$$P_{B_{tr}}^{kin} = KB(B^T B)^{-1} B^T K^{-1}, \quad P_{a_{tr}}^{kin} = Ga(a^T a)^{-1} a^T G^{-1} \quad (19)$$

$$K = \begin{bmatrix} R & RL \\ 0 & R \end{bmatrix}, \quad G = \begin{bmatrix} R & 0 \\ RL & R \end{bmatrix}, \quad (20)$$

where $P_{B_{tr}}^{kin}$ and $P_{a_{tr}}^{kin}$ are the kinestatic filters after a transformation was applied to the compliant frame, L a skew-symmetric matrix associated with a translation vector and R is a rotation of the compliant frame [20]. For a translation of a distance d in the x -axis direction $R = I_3$ and $L = \begin{bmatrix} 0 & 0 & 0 \\ 0 & 0 & -d \\ 0 & d & 0 \end{bmatrix}$, cf. with Fig. 1, the kinestatic filters in Eq. (13) are

$$P_{B_{tr}}^{kin} = \begin{bmatrix} 0 & 0 & 0 & 0 & 0 & 0 \\ 0 & 0 & 0 & 0 & 0 & -d \\ 0 & 0 & 1 & 0 & -d & 0 \\ 0 & 0 & 0 & 0 & 0 & 0 \\ 0 & 0 & 0 & 0 & 0 & 0 \\ 0 & 0 & 0 & 0 & 0 & 1 \end{bmatrix}, \quad P_{a_{tr}}^{kin} = \begin{bmatrix} 1 & 0 & 0 & 0 & 0 & 0 \\ 0 & 1 & 0 & 0 & 0 & 0 \\ 0 & 0 & 0 & 0 & 0 & 0 \\ 0 & 0 & 0 & 1 & 0 & 0 \\ 0 & 0 & d & 0 & 1 & 0 \\ 0 & d & 0 & 0 & 0 & 0 \end{bmatrix}. \quad (21)$$

For the same transformation, if Eq. (19) are applied to the filters defined in Eq. (18), they become

$$P_{B_{tr}} = \begin{bmatrix} 0 & 0 & 0 & 0 & 0 & 0 \\ 0 & d^2/d^2 + 1 & 0 & 0 & 0 & -d/d^2 + 1 \\ 0 & 0 & 1 & 0 & 0 & 0 \\ 0 & 0 & 0 & 0 & 0 & 0 \\ 0 & 0 & 0 & 0 & 0 & 0 \\ 0 & -d/d^2 + 1 & 0 & 0 & 0 & 1/d^2 + 1 \end{bmatrix}, \quad (22)$$

$$P_{a_{tr}} = \begin{bmatrix} 1 & 0 & 0 & 0 & 0 & 0 \\ 0 & 1/d^2 + 1 & 0 & 0 & 0 & d/d^2 + 1 \\ 0 & 0 & 0 & 0 & 0 & 0 \\ 0 & 0 & 0 & 1 & 0 & 0 \\ 0 & 0 & 0 & 0 & 1 & 0 \\ 0 & d/d^2 + 1 & 0 & 0 & 0 & d^2/d^2 + 1 \end{bmatrix}. \quad (23)$$

To test if $P_{B_{tr}}^{kin}$, $P_{a_{tr}}^{kin}$, $P_{B_{tr}}$ and $P_{a_{tr}}$ correctly filter out commanded twists except for \mathbf{T}_3 and \mathbf{T}_6 , we command an

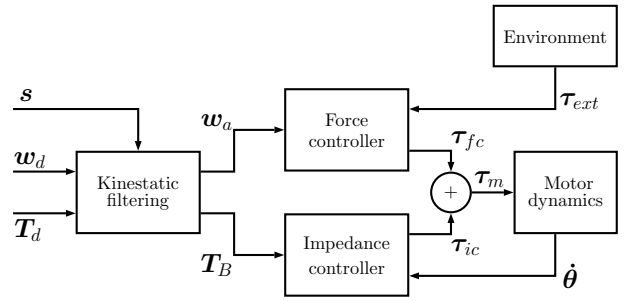


Fig. 3: System overview. Desired wrench ω_d and motion T_d are projected to the mutually consistent values w_a and T_B according to a task description s and only then commanded to the force and impedance controllers.

elementary pseudo-twist $\mathbf{T}'_5 = K\mathbf{T}_5 = [0 \ 0 \ d \ 0 \ 1 \ 0]^T$. The filtered pseudo-twists are

$$T_{P_{B_{tr}}^{kin}} = P_{B_{tr}}^{kin} \mathbf{T}'_5 = [0 \ 0 \ 0 \ 0 \ 0 \ 0]^T, \quad (24)$$

$$T_{P_{B_{tr}}} = P_{B_{tr}} \mathbf{T}'_5 = [0 \ 0 \ d \ 0 \ 0 \ 0]^T. \quad (25)$$

Since the task description only allows for motions in $KB = \{K\mathbf{T}_3, K\mathbf{T}_6\}$, we can see from Eq. (24), the commanded motion \mathbf{T}'_5 is successfully filtered out by $P_{B_{tr}}^{kin}$. On the other hand filter $P_{B_{tr}}$, see Eq. (25), yields an undesired translation of d along the z -axis, resulting from the use of the selection matrix and thus is noninvariant.

IV. PRACTICAL CONSIDERATIONS

A. Selection vector

In order to design the filters P_B and P_a , the task description needs to be carefully defined through matrices B and a , as exemplified in Sec. III-C. We abstract the environment description from the end-user by defining an interface variable that resembles the selection matrix: the *selection vector* $s \in \mathbb{R}^6$. Where a “1” indicates that the given direction is force-controlled, e.g. force and torque control along the x - and y -axis respectively $s = [1, 0, 0, 0, 1, 0]^T$, while translational motion can be performed in directions y , z and rotations about axes x , z . From this selection vector the environment model a , B are generated automatically. Then, the kinestatic filters P_a , P_B and the consistent twist and wrench T_B , w_a are calculated. Therefore, only consistent commands are used as desired values for the force-tracking augmented impedance controller, as depicted in Fig. 3.

B. Saturation and loss of contact

A common issue for force-control schemes is the instability induced by contact loss and/or saturation. The former is caused by uncertainties and changes in the environment, while the latter is due to the integral component of the controller winding-up beyond the actuator limits. Concerning this issue we use an anti-aliasing mechanism with a tunable maximum value for the integral wrench error

$$\text{if } \Delta_f(t)^{Int} > val_{max} \wedge \Delta_f(t) > 0 \text{ then} \\ \Delta_f(t) \leftarrow 0$$

else if $\Delta_f(t)^{Int} < -val_{max} \wedge \Delta_f(t) < 0$ **then**
 $\Delta_f(t) \leftarrow 0$
else
 $\Delta_f(t) \leftarrow \mathfrak{F}_{ext}(t) - \mathfrak{F}_d(t)$
end if

where $\Delta_f(t)^{Int} = K_i \int \Delta_f(t) dt$, for convenience. The first two conditions enforce a null integral component for the windup effect w.r.t to maximum allowed value, as long as val_{max} is itself less or equal to the torque saturation thresholds. This limits the robot motion in case contact was lost along the force-constrained axis. However, the allowed robot motion is a consequence of the limitation on the integral wrench error and represents only a pragmatic solution. Next, the designed system and the practical solutions we developed are validated in experiments.

V. EXPERIMENTAL RESULTS

The experimental setup consists of the LWR, a 6-DOF force/torque sensor attached to its wrist and a surface of contact. Firstly, the characteristics of the motion, which is commanded by a high-level planner are described in Sec. V-A. Then, the kinestatic filter is applied through the selection vector with a zero desired wrench in Sec. V-B. Finally, a non-zero wrench is applied simultaneously with the motion and the system's force-tracking capabilities and response to disturbances are interpreted in Sec. V-C.

A. Unconstrained motion

The commanded path comprises a cyclic Cartesian trajectory of three points. The starting position is denoted S . When the motion starts the robot moves from position S to the first point 1, continues to 2 then 3, completing the cycle at position 1 again, then, the motion is repeated, see Fig. 4a. All values are specified in the frame of the robot's base located at $(0, 0, 0)$, and are shown in Tab. I and in Fig. 4b. For sake of simplicity rotation components are left constant between points.

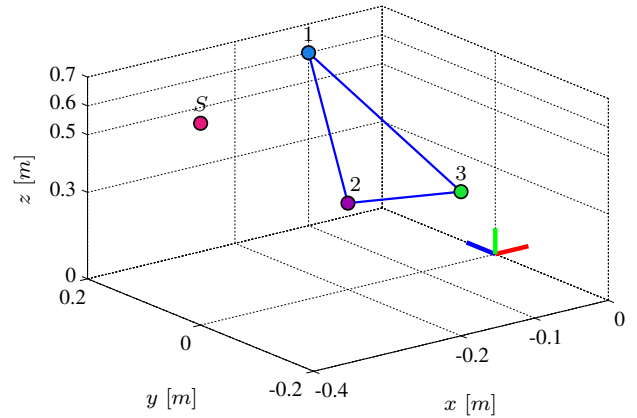
TABLE I: Numerical values for a cyclic Cartesian trajectory.

	S	1	2	3
x	-0.4	-0.1	-0.2	-0.2
y	0.0	0.2	0.0	-0.2
z	0.7	0.6	0.3	0.5

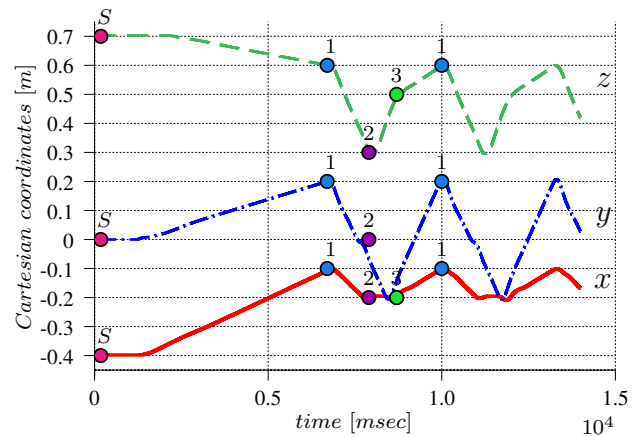
B. Motion filter with zero-wrench

We use the selection vector as a straight-forward way to generate filters that project the desired motion and wrench onto a consistent subspace. If the selection vector were chosen as $s_x^F = [1, 0, 0, 0, 0, 0]^T$, then a force along the x -axis is to be performed, analogously for s_y^F and s_z^F . This means that a *motion command* cannot be executed² and thus should be filtered out. On the other hand, $s_z^\tau = [0, 0, 0, 0, 0, 1]^T$ denotes that the z -axis is torque-constrained. If the desired

²The robot will have a motion as to push the contact surface and reach the desired force, but this is a consequence of the force set point, not of a commanded position.



(a) The motion starts at position S . The robot moves to point 1 and then a cyclic trajectory through points 2, 3 and 1 is performed.



(b) Free-motion trajectory vs. time. This representation is used hereafter as the components of the trajectory can be easily seen to change over time.

Fig. 4: Desired motion as a cyclic trajectory shown as an spatial representation a) and as a sequence in time b).

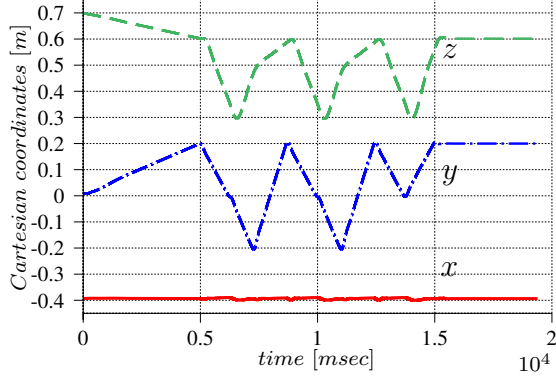
wrench has a value of zero the motion is performed without exerting a wrench, and the motion along of one of the axis will be constrained as shown in Fig. 5. Here, the desired motion is effectively filtered out along the force-controlled axes and the starting position is kept constant, cf. Fig. 4b.

C. Simultaneous wrench and motion command

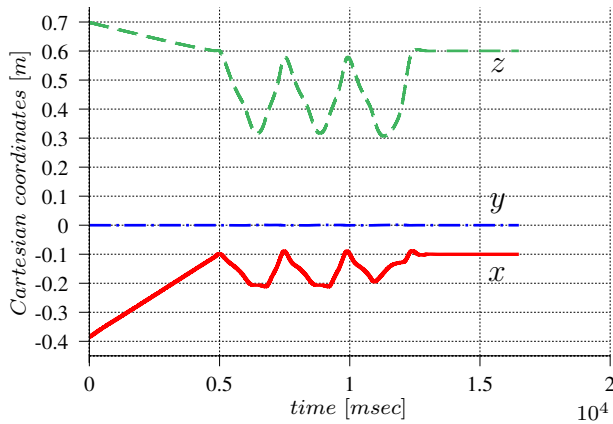
In the following experiments, the desired cyclic motion is commanded as well as a force of 10 [N] along x - and z -axis. Four segments are differentiated on the plots in Fig. 6. Namely, motion before contact and the start of contact with the surface, I , sustained force and external disturbance $II - III$ and loss of contact IV . In the case of a force applied along the x -axis, the robot moves in the negative x direction until contact is achieved, see Fig. 6a. A disturbance was applied along this axis pushing the robot, thus, increasing the contact force up to 15 [N]. Since a value of 10 [N] was commanded, the robot counteracts the disturbance in order to decrease the contact force, section II . After the

TABLE II: Numerical values for the impedance controller

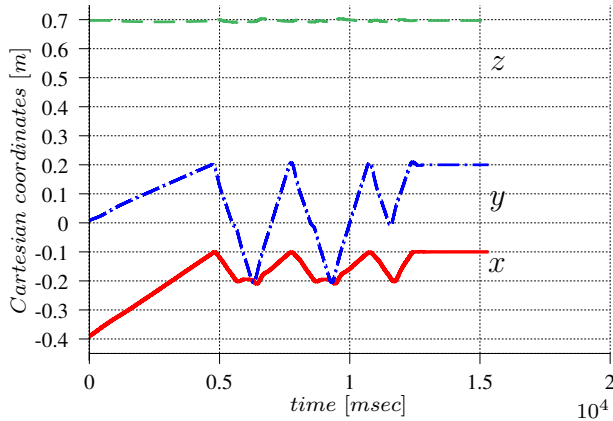
		${}^x K_x$ [N/m]	${}^z K_x$ [N/m]	D_x [Ns/m]
trans	x	500	1500	0.7
	y	1500	1500	0.7
	z	1500	500	0.7
rot	x	200	200	0.7
	y	200	200	0.7
	z	200	200	0.7



(a) Desired trajectory with $\mathbf{s}_x^F = [1, 0, 0, 0, 0, 0]^T$ and a zero-wrench applied to the environment. The motion along x -axis is properly filtered out.



(b) The constrained motion along y -axis is the result of a zero-wrench specification and a selection vector $\mathbf{s}_z^F = [0, 1, 0, 0, 0, 0]^T$.



(c) In the case when $\mathbf{s}_z^F = [0, 0, 1, 0, 0, 0]^T$, the motion along the z -axis should be filtered. As seen from the plot, the z -axis remains at the same value of the starting position S , namely 0.7.

Fig. 5: For these experiments a zero-wrench was commanded with three different selection vector \mathbf{s}_x^F , \mathbf{s}_y^F and \mathbf{s}_z^F . Therefore, the specified axis is wrench-constrained and a motion should not be performed along those axes.

external disturbance is lifted, the controller tracks the desired force until the surface is moved and contact is lost. Here, anti-windup is not enabled and the robot moves further until contact is regained, or threshold limits are reached.

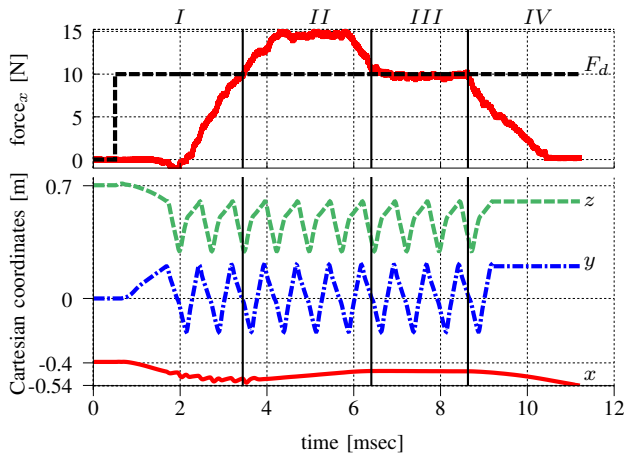
For the experiment shown in Fig. 6b, the robot comes in contact with the environment in segment II. Then, a disturbance is applied along the z -axis. After a few moments, the disturbance is lifted and the robot seeks contact again. With anti-windup and after loss of contact the robot will move until the limiting threshold is reached, in this case it moves ≈ 20 [cm] from the starting point, which is an indirect limit imposed by the anti-windup approach.

Relevant values used for the force controller and also for the impedance controller are shown in Tab. II. Where ${}^x K_x$ denotes the spatial Cartesian stiffness for the experiment with desired force along x -axis, and ${}^z K_x$ along z -axis. The stiffness is decreased for the respective experiments, otherwise the response of the controller is slower. This is due to the opposing action of the virtual spring along x or z that the controller needs to overcome in addition to the surface contact force.

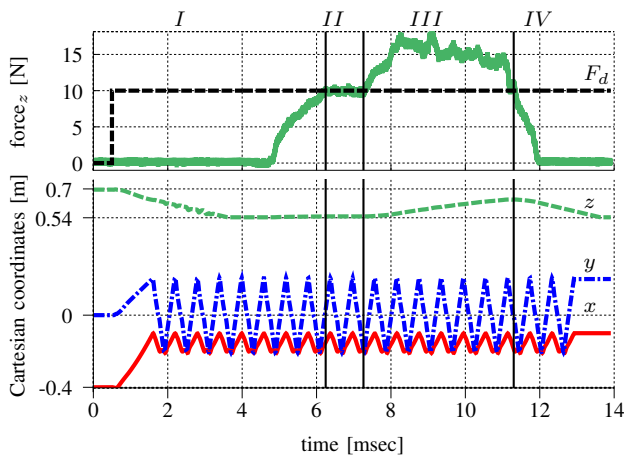
VI. CONCLUSIONS AND DISCUSSION

In this paper we designed a novel system for simultaneous wrench and position specification. The system is composed of an impedance controller, used for Cartesian motion, on top of which an explicit force-feedback loop was designed. The unified system is characterized by compliance as well as the possibility to achieve a desired wrench value. Commanded motion and wrench are guaranteed to be consistent with each other and the task model. This is achieved by means of a kinematic filter, that projects inconsistent motion/wrench commands onto a consistent subspace, effectively filtering out undesired motions even if the compliant frame undergoes rigid transformations. We simplified the task model specification by introducing a 6D selection vector, from which the more evolved task model is inferred, and thereafter the projection matrices. Experiments were carried out in order to show independent filtering specifications. Also an empirical approach to contact loss was presented in the form of an anti-windup technique.

However, there are issues to keep in mind when dealing with kinematic filtering. Even though the compliant frame can always be determined, on some cases it might *not be unique*, which in turn renders the filters non-unique. Also, if the metrics are preserved under Euclidean transformations then $\Psi = K^{-T} \Psi K^{-1}$ and $\psi = G^{-T} \psi G^{-1}$, but no positive



(a) Constrained motion with desired force along x-axis. A disturbance is applied to the robot and it tries to regulate to force by moving away from contact. As soon as it is lifted the robot starts moving forward to re-gain contact.



(b) Constrained motion with desired force along z-axis. A disturbance is applied to the robot and it tries to regulate to force by moving away from contact. Once the disturbance disappears the robot tries to regain contact, but it is limited by the max distance it can move from its starting point at 0.7 [m].

Fig. 6: An inconsistent motion is commanded along a desired force value $F_d = 10$ [N]. The commanded motion along the force-constrained axes is filtered out and the desired force is achieved.

definite matrix satisfies these equations [21]. The solution is to account for the transformation as in Eq.(15) and the decomposition is made invariant for non-Euclidean metrics [13]. But a method which does not rely on metric invariance can be more general and handy, an outlook into this issue as well as a more refined comparison practical uses of different approaches are left for future work.

REFERENCES

- [1] W. Wang, R. N. Loh, and E. Y. Gu, "Passive compliance versus active compliance in robot-based automated assembly systems," *Industrial Robot: An International Journal*, vol. 25, no. 1, pp. 48–57, 1998.
- [2] J. J. Craig and M. H. Raibert, "A systematic method of hybrid position/force control of a manipulator," in *Computer Software and*

- Applications Conference, 1979. Proceedings. COMPASAC 79. The IEEE Computer Society's Third International*, pp. 446–451, 1979.
- [3] O. Khatib, "A unified approach for motion and force control of robot manipulators: The operational space formulation," *Robotics and Automation, IEEE Journal of*, vol. 3, no. 1, pp. 43–53, 1987.
- [4] M. T. Mason, "Compliance and force control for computer controlled manipulators," *Systems, Man and Cybernetics, IEEE Transactions on*, vol. 11, no. 6, pp. 418–432, 1981.
- [5] H. Lipkin and J. Duffy, "Hybrid twist and wrench control for a robotic manipulator," *Journal of Mechanical Design*, vol. 110, no. 2, pp. 138–144, 1988.
- [6] F. Lange, W. Bertleff, and M. Suppa, "Force and trajectory control of industrial robots in stiff contact," in *Robotics and Automation (ICRA), 2013 IEEE International Conference on*, pp. 2927–2934, IEEE, 2013.
- [7] F. Lange, C. Jehle, M. Suppa, and G. Hirzinger, "Revised force control using a compliant sensor with a position controlled robot," in *Robotics and Automation (ICRA), 2012 IEEE International Conference on*, pp. 1532–1537, IEEE, 2012.
- [8] G. Ferretti, G. Magnani, and P. Rocco, "Toward the implementation of hybrid position/force control in industrial robots," *Robotics and Automation, IEEE Transactions on*, vol. 13, no. 6, pp. 838–845, 1997.
- [9] T. Kröger, B. Finkemeyer, M. Heuck, and F. M. Wahl, "Adaptive implicit hybrid force/pose control of industrial manipulators: Compliant motion experiments," in *Intelligent Robots and Systems, 2004.(IROS 2004). Proceedings. 2004 IEEE/RSJ International Conference on*, vol. 1, pp. 816–821, IEEE, 2004.
- [10] L. Cai and A. Goldenberg, "An approach to force and position control of robot manipulators," in *Robotics and Automation, 1989. Proceedings., 1989 IEEE International Conference on*, pp. 86–91, IEEE, 1989.
- [11] M. H. Raibert and J. J. Craig, "Hybrid position/force control of manipulators," *Journal of Dynamic Systems, Measurement, and Control*, vol. 103, no. 2, pp. 126–133, 1981.
- [12] C. Schindlbeck and S. Haddadin, "Unified passivity-based cartesian force/impedance control for rigid and flexible joint robots via task-energy tanks," *Robotics and Automation (ICRA), 2015 IEEE International Conference on*, 2015.
- [13] A. Abbati-Marescotti, C. Bonivento, and C. Melchiorri, "On the invariance of the hybrid position/force control," *Journal of Intelligent and Robotic Systems*, vol. 3, no. 3, pp. 233–250, 1990.
- [14] G. Hirzinger, N. Sporer, A. Albu-Schaffer, M. Hahnle, R. Krenn, A. Pascucci, and M. Schedl, "DLr's torque-controlled light weight robot iii-are we reaching the technological limits now?," in *Robotics and Automation, 2002. Proceedings. ICRA'02. IEEE International Conference on*, vol. 2, pp. 1710–1716, IEEE, 2002.
- [15] M. W. Spong, S. Hutchinson, and M. Vidyasagar, *Robot modeling and control*, vol. 3. Wiley New York, 2006.
- [16] N. Hogan, "Impedance control: An approach to manipulation," in *American Control Conference, 1984*, pp. 304–313, IEEE, 1984.
- [17] A. Albu-Schäffer, C. Ott, and G. Hirzinger, "A unified passivity-based control framework for position, torque and impedance control of flexible joint robots," *The International Journal of Robotics Research*, vol. 26, no. 1, pp. 23–39, 2007.
- [18] S. Stramigioli and V. Duindam, "Variable spatial springs for robot control," 2001.
- [19] S. Chiaverini, B. Siciliano, and L. Villani, "A stable force/position controller for robot manipulators," in *Decision and Control, 1992., Proceedings of the 31st IEEE Conference on*, pp. 1869–1874, IEEE, 1992.
- [20] H. Lipkin and J. Duffy, "The elliptic polarity of screws," *Journal of Mechanisms, Transmissions, and Automation in Design*, vol. 107, no. 3, pp. 377–386, 1985.
- [21] J. Loncaric, *Geometrical Analysis of Compliant Mechanisms in Robotics (Euclidean Group, Elastic Systems, Generalized Springs)*. PhD thesis, Cambridge, MA, USA, 1985. AAI8520241.